Proceedings World Geothermal Congress 2023
Beijing, China, April 17 – 21, 2023

Study of fracture initiation and propagation in HDR based on true triaxial experiment in high temperature

Li Runsen[1], Hou Bing[1*], Derek Elsworth[2], Zhuang Li[3]

1. State Key Laboratory of Resources and Prospecting, China University of Petroleum, Beijing 102249, China

2. The Pennsylvania State University, University Park, PA, 16802, USA

3. Korea Institute of Civil Engineering and Building Technology, Goyang, Republic of Korea

lrunsen@126.com, binghou@vip.163.com, elsworth@psu.edu, zhuangli@kict.re.kr

Keywords: Hot dry rock; Fracture intersection behavior; High-temperature; True triaxial hydraulic fracturing

ABSTRACT

At present, the main way to exploit hot dry rock (HDR) is to inject the low-temperature working fluid into the high-temperature formation, and then extract the geothermal resources after heating. Hydraulic fracturing of HDR reservoirs is an important technique to increase geothermal production. Compared with normal temperature reservoir, temperature is an important factor that can not be ignored in the fracturing of HDR reservoir, and the complex multi-field coupling caused by temperature change is difficult to be realized by numerical modeling method at present. In this paper, the effects of temperature, in-situ stress and fracturing fluid injection rate during fracturing were investigated with the help of custom-built, heated, large-scale true triaxial hydraulic fracturing equipment. The results show that temperature influences fracture pressure and brittleness of rock. The higher the temperature, the lower the fracture pressure and the weaker the brittleness. The influence of in-situ stress and fluid injection velocity on HDR reservoir is similar to the influence of normal temperature formation fracturing. The experience and method of normal temperature reservoir fracturing design can be referred to in the design of HDR reservoir fracturing.

1. INTRODUCTION

Hot dry rock (HDR) is a kind of geothermal resource with reservoir depth of about 3~10 km and stratum temperature of about 150~650 ℃[1, 2]. The hot dry rock reservoir is mostly granite, and there is no water or steam in the hot rock. It is the most potential and valuable part of geothermal energy[3]. Due to the deep buried depth of HDR reservoir, the large overburden pressure makes the reservoir porosity and permeability usually low, which makes the direct exploitation difficult and low economic benefits. Hydraulic fracturing improves the flow conductivity of granite and makes it meet the conditions of industrial exploitation. However, granite has a low content of clay minerals and strong brittleness, so it is easy to form natural fractures with different angles under the high in-situ stress field. If natural fractures can be rationally utilized in the fracturing process to communicate with hydraulic fractures to form a complex fracture network, the SRV can be significantly expanded and production can be increased.

In view of this situation, scholars have conducted extensive research. Yoshida K., Fomin S. et al. (2004) pointed out that hydraulic fracturing is one of the most effective methods to improve the productivity of HDR[4]. They used the fractal geometric network model to randomly generate a serise of fractures in space and established a mathematical model for hydraulic fracturing of dry hot rock. Zhang (2014) further developed the temperature-seepage-stress-damage (THMD) multi-field coupling simulation program by using FISH+FORTRAN language, which provided theoretical basis and method for numerical simulation of this problem[5]. Based on laboratory tests, Guo (2016) established hydraulic fracture initiation, propagation and rock damage models, and considered the influence of temperature on rock strength[6]. Zhou et al. (2018) took Shandong gray granite as the experimental object and conducted hydraulic fracturing experiments at different temperatures, and found that the splitting pressure decreased significantly at high temperatures[7]. Then, a transient thermo-mechanical coupling model was established to simulate the near-wellbore area, and it was pointed out that the influence mechanism of temperature on granite hydraulic fracturing was not the change of rock mechanical parameters, but the thermal shock caused by the action of rock fracturing fluid at high temperature. Hou et al. (2021)[8, 9], Chang et al. (2022)[10], Dai et al. (2021)[11-14], Zhang et al. (2021)[13, 14] simluate the intersection behavior of hydraulic fractures and natural fractures under different geological conditions by using mainstream numerical simulation algorithms such as finite element method, discrete element method, phase field method and DFN, and pointed out that the intersection of hydraulic fractures and natural fractures is mainly affected by the difference of in-situ stress and angle. Jin et al. (2020) used a special true three-axis hydraulic fracturing test system to conduct numerical simulation of hydraulic fracturing in granite outcrops in Gonghe Basin, Qinghai Province under real stratigraphic environment, which provided guidance for designing and evaluating hydraulic fracturing operations in HDR geothermal formations[15-18].

In this paper, the true triaxial hydraulic fracturing experiment is carried out under high temperature environment, and the laws of fracture initiation, extension and intersection with natural fractures during HDR stratum fracturing are studied. The experimental method overcomes the shortcomings of simulating formation temperature through heat treatment in the past, and the obtained laws are more accurate and more instructive for HDR reservoir hydraulic fracturing operation.

2. HYDRAULIC FRACTURING EXPERIMENT OF HDR

In order to study the fracture morphology and fracture propagation law of HDR reservoir, 8 sets of true triaxial hydraulic fracturing experiments were carried out. A custom-built large-scale true triaxial simulation system was used, on which a heating thermostat system was installed to heat the samples during the experiment. The heating thermostat system is equipped with three heating rods with a power of 2000W and a temperature sensor on each surface except the bottom surface of the rock sample, these components can ensure that the temperature of HDR reservoir is heated uniformly at the set heating rate and stratum temperature is accurately simulated in the experiment, experiment equipment diagram as shown in the figure below.

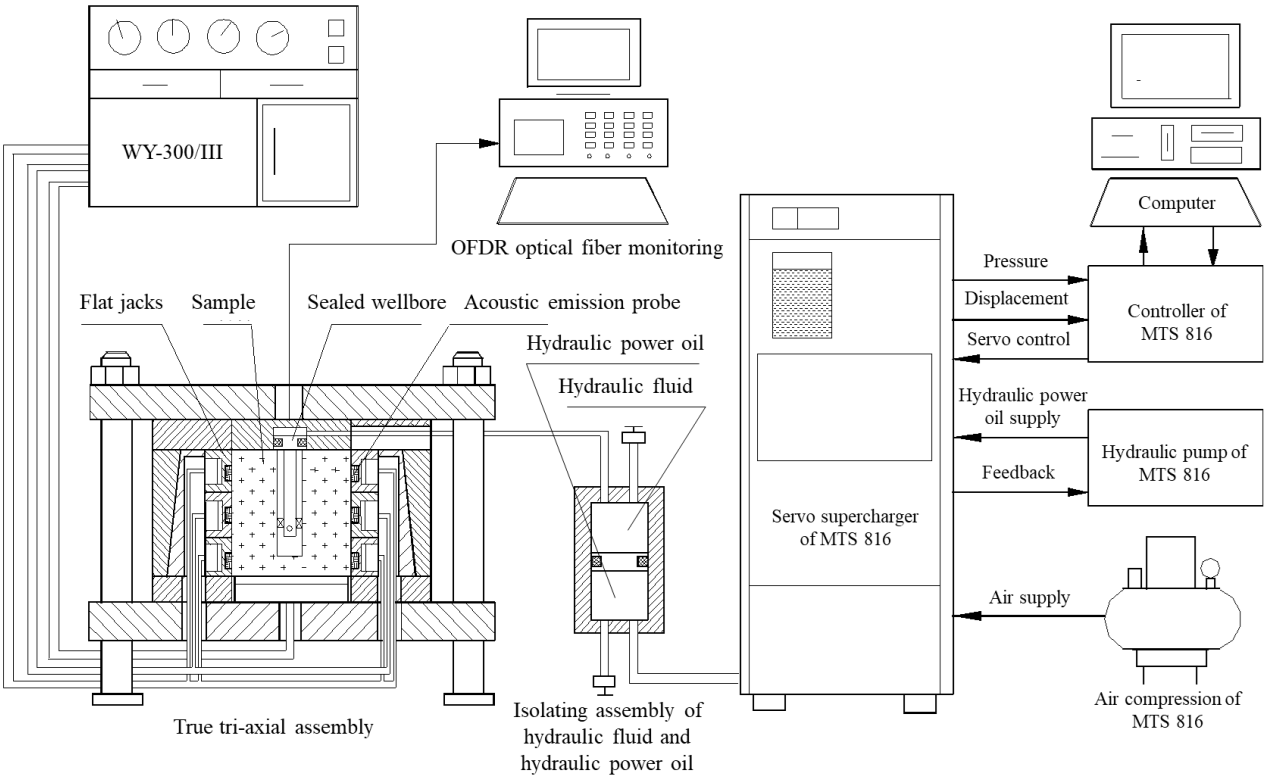

Fig.1 Experiment equipment diagram

The rock samples used in the experiment are granite wild outcrops with a size of 300mm×300mm×300mm, as shown below. The rock samples were taken from Gonghe Basin, Qinghai Province, China. The proven reserves of HDR in this area are about 630.3 billion tons of standard coal, which is one of the core areas for HDR mining. Before the experiment, a drilling machine was used to drill a small hole in the middle of one face of the dry hot rock sample, and a metal tube with high temperature and pressure resistance was inserted to simulate the fracturing wellbore, and the sealing ring and sealant were used for sealing treatment. Then the HDR sample was put into the chamber of the true three-axis hydraulic fracturing equipment for heating. A temperature sensor is installed in the fracturing wellbore in the middle of the rock sample. When the internal temperature and surface temperature of the rock sample become the same, it is proved that the rock sample has reached the temperature set by the experiment. After that, the temperature was kept constant and the fracturing experiment began.

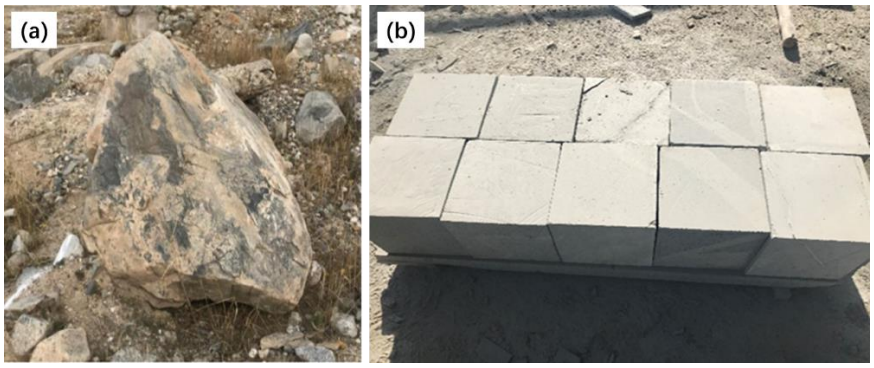

Fig.2 Experiments used granite outcrops and rock samples taken from Gonghe Basin. (a): granite outcrops get from wild without any treatment; (b): granite samples with a size of 300mm×300mm×300mm cut from outcrops

A total of 8 groups of fracturing experiments were conducted, and several representative sets of parameters were selected within the test capability of the experimental equipment to experimentally study the HDR fracture propagation under different temperatures, confining pressures, injection rates and viscosity. The experimental parameters are shown in Table 1 below.

Table 1 Parameters used in experiments

Index	Temperature (℃)	Confining pressure (h/H/v) (MPa)	Injection rate (ml/min)	Viscosity (mPa·s)
1#	120	7/10/15	30	33.1
2#	120	7/13/15	30	1
3#	200	7/10/15	30	33.1
4#	200	7/10/15	30	1
5#	200	7/13/15	5	33.1
6#	200	7/13/15	30	1
7#	200	7/13/15	10	33.1
8#	200	7/13/15	30	33.1

3. DISCUSSION

3.1 Fracturing under different stratum temperature

Compared with ordinary formation hydraulic fracturing, the temperature of HDR reservoir is higher and the temperature change is more obvious during fracturing. The resulting change in rock's physical and mechanical properties has a non-negligible impact on fracture extension. The existing researches usually believe that high temperature will produce thermal stress, which will reduce the rock fracture pressure. In fact, temperature change will also affect the brittleness of rock, directly affect the mechanical behavior of rock before failure, and then affect the formation of cracks. This is the result of coupling of multiple physical fields, which is difficult to be accurately described by numerical simulation. Therefore, a true triaxial fracturing experiment at high temperatures is the most reliable method to determine the effect of temperature on the fracturing of HDR.

Compare rock samples 1#, 2#, 3# and 6#, the experimental parameters are shown in the following table. Among them, 1# and 3# were fractured with guar gum fracturing fluid system (33.1 MPa.s) under a large stress difference (5MPa), and 2# and 6# were fractured with slickwater fracturing fluid (1 MPa.s) under a small stress difference (2MPa).

Table 2 Experiments parameters used for rock samples 1#、2#、3# and 6#

Index	Temperature (℃)	Confining pressure (h/H/v) (MPa)	Injection rate (mL/min)	Viscosity (mPa·s)
1#	120	7/10/15	30	33.1
2#	120	7/13/15	30	1
3#	200	7/10/15	30	33.1
6#	200	7/13/15	30	1

Fig. 3 shows the fracture morphology and schematic diagram of rock sample 6# after fracturing. The rock sample # 6 is formed by concrete pouring and basically belongs to isotropic, homogeneous and complete rock samples. When slickwater is used as fracturing fluid at 200℃, the fracture expands along the direction of maximum in-situ stress in the plane, forming a typical hydraulic fracture. Due to the particularity of concrete rock samples, there is no special case of crack turning, and the crack surface is relatively smooth. The situation with natural outcrop fracturing is more complicated.

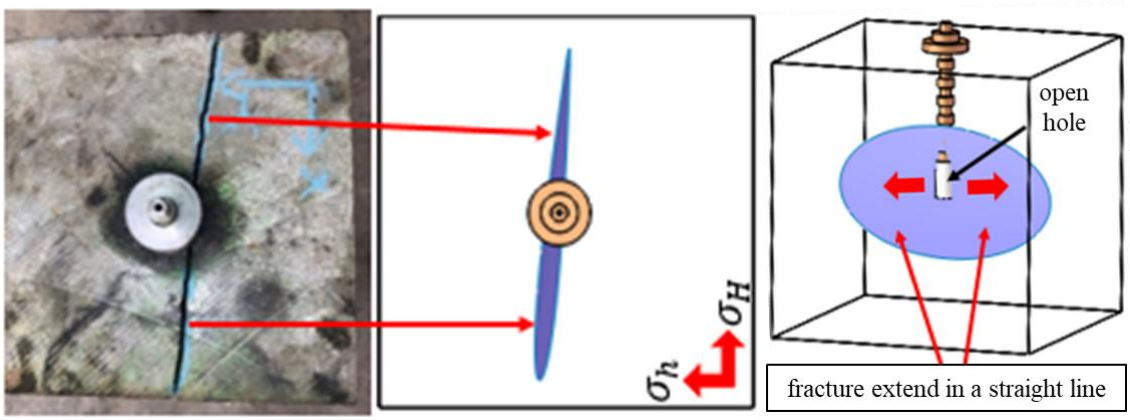

Fig.3 Photo after fracturing and three-dimensional diagram after fracturing of rock sample 6#. (a): Photo of the fracture surface after fracturing; (b): Top view of rock sample 6# after fracturing; (c): 3D perspective view of rock sample 6# after fracturing.

The fracture morphology and 3D reconstruction of rock sample 1# after the experiment are shown in Fig.4. The 1# sample was fractured at 120 ° C using a fracturing fluid with a viscosity of 33.1 mPa·s. There is a vertical natural fracture in the lower part of the open hole section, which directly communicates with the wellbore. Instead of starting from the open hole section, the fracture in sample 1# started directly at the natural fracture and then extend along the natural fracture at the bottom of the wellbore. The fracture area formed was small and failed to penetrate the surface of the rock sample.

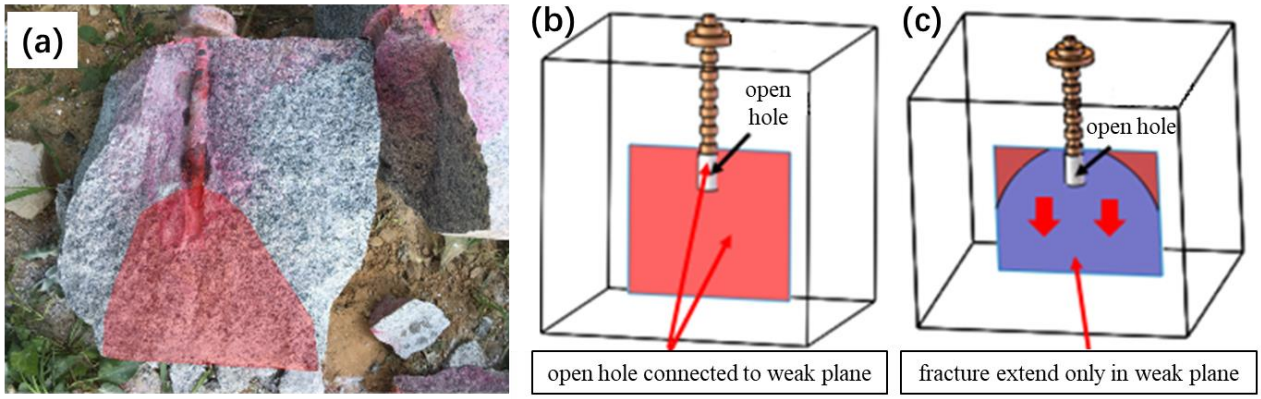

Fig.4 Photo after fracturing and three-dimensional diagram before and after fracturing of rock sample 1#. (a): Photo of the fracture surface after fracturing, in which the purple on the rock sample is colored fracturing fluid; The red areas are natural fractures; (b): Schematic diagram of artificial wellhead and natural fractures before fracturing; (c): Schematic diagram of artificial wellhead and natural fractures after fracturing;

The fracture morphology and 3D reconstruction of rock sample 2# after the experiment are shown in Fig.5. The 2# sample was fractured at 120 ° C using a fracturing fluid with a viscosity of 1 mPa·s. Sample 2 # after fracturing cracks appear obvious deflection. However, no natural fractures or dikes were observed on the surface before fracturing, and the fracturing curve also showed that there were no large natural fractures, and the difference in plane in-situ stress during fracturing was larger. These indicate that the HDR samples have strong heterogeneity, and even the outcrops obtained in the same area may have obvious differences in their properties.

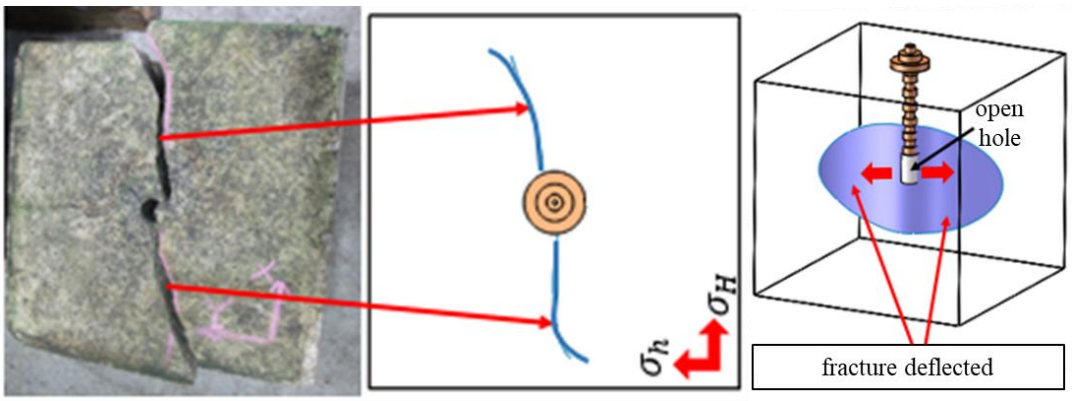

Fig.5 Photo after fracturing and three-dimensional diagram after fracturing of rock sample 2#. (a): Photo of the fracture surface after fracturing; (b): Top view of rock sample 3# after fracturing; (c): 3D perspective view of rock sample 3# after fracturing.

The fracture morphology and 3D reconstruction of rock sample 3# after the experiment are shown in Fig.6. The 3# sample was fractured at 200 ° C using a fracturing fluid with a viscosity of 33.1 mPa·s. In Fig.6 (a), it can be seen that there are inclined bedding and dikes of about 45 degrees in rock sample 3#, and the fracture obviously deflects in the direction of bedding during fracturing.

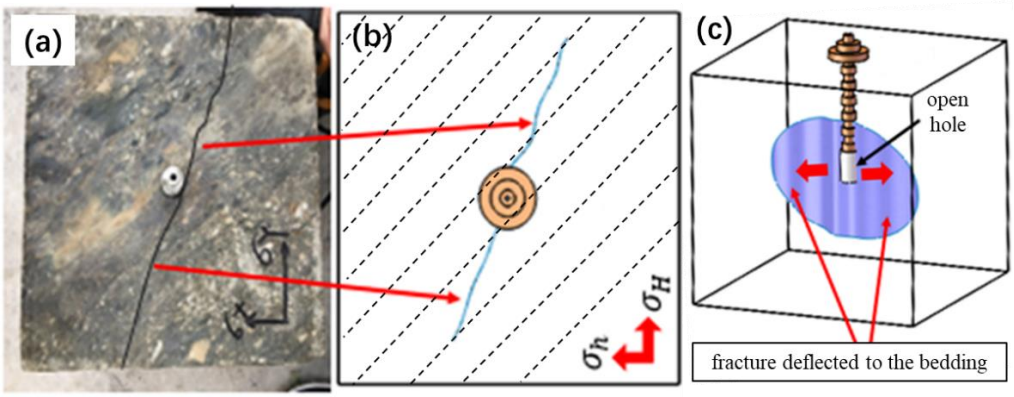

Fig.6 Photo after fracturing and three-dimensional diagram after fracturing of rock sample 3#. (a): Photo of the fracture surface after fracturing; (b): Top view of rock sample 3# after fracturing; (c): 3D perspective view of rock sample 3# after fracturing.

Fig.7 shows the fracturing curves of rock samples 1#, 2# and 3#. Both 1# and 3# curves in the figure have a 2-3min pressure stage of 0MPa, which is caused by natural fractures inside the sample directly connected to the open hole section of the artificial wellhead. Comparing the curves of rock sample 1# and rock sample 3# in the figure shows that the temperature has a certain effect on the fracture pressure of dry hot rock when guar gum is used as fracturing fluid. With the increase of temperature, the fracture pressure decreases, which is also consistent with the results of theoretical analysis. The fracture pressure at 120℃ (1# rock sample) is about 27.7MPa, and that at 200℃ (3# rock sample) is about 22.5MPa. Meanwhile, at the same injection rate, the pressure increment per unit time before fractured of the curve at 200℃ in the figure is significantly smaller than that at 120℃. This indicates that the brittleness of rocks decreases with the increase in temperature. By comparing the curves of the 1# and 2# rock samples, the 1# rock sample has natural fractures at the bottom of the open hole section, and the overall strength decreases, but its fracture pressure is higher than that of the 2# rock sample without natural fractures, indicating that the smaller the fracturing fluid viscosity at the same temperature, the smaller the fracture pressure.

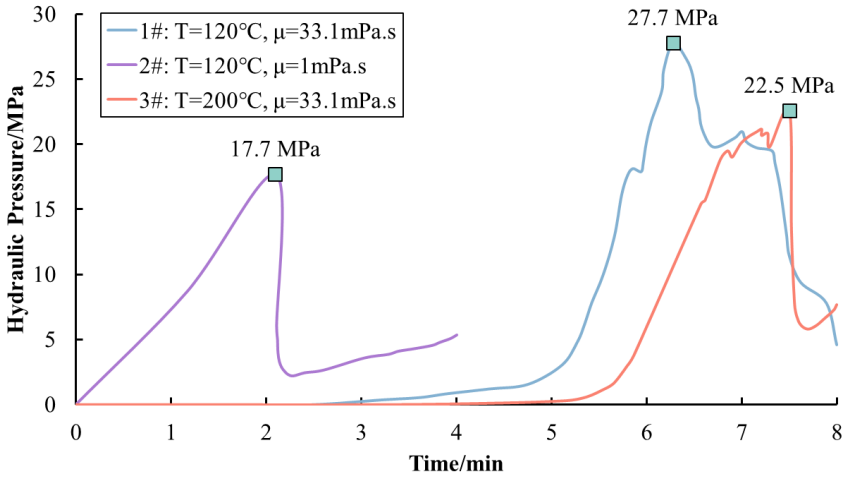

Fig.7 Hydraulic pressure curve of rock sample 1#, 2# and 3# during fracturing

3.2 Fracturing under different confining pressure

A large number of research results show that the difference of in-situ stress has a great influence on fracture propagation, which is reflected in the fact that the propagation direction of fractures in homogeneous and isotropic strata is controlled by the direction of maximum in-situ stress. The intersection behavior of hydraulic fracture and natural fracture is affected by the difference of in-situ stress. And the volume fracture size is affected by the difference of stress. In the experiment, confining pressure is applied by real triaxial equipment to simulate real in-situ stress environment. The parameters used in the simulation are shown in Table 3 below.

In order to study the influence of in-situ stress on fracturing fracture development of HDR under high-temperature environment, four groups of experiments were carried out at 200℃ with vertical confining pressure and horizontal minimum pressure of 15MPa and 7MPa respectively. The plane maximum pressure of four rock samples was 13MPa and 10MPa respectively, and the fracturing fluid was guar gum and slickwater. The parameters used in the simulation are shown in Table 3 below.

Table 3 Experiments parameters used for rock samples 3#、4#、6# and 8#

Index	Temperature (℃)	Confining pressure (h/H/v) (MPa)	Injection rate (mL/min)	Viscosity (mPa·s)
3#	200	7/10/15	30	33.1
4#	200	7/10/15	30	1
6#	200	7/13/15	30	1
8#	200	7/13/15	30	33.1

The post-fracturing photo of 4# rock sample and the three-dimensional diagram of fracture surface are shown in Fig.8 below. The fracture expands along the direction of maximum stress in the horizontal direction, and the fracture morphology is relatively simple. Compared with the 6# rock sample, the 4# rock sample has a smaller stress difference in plane, and the fracture surface after fracturing is obviously rougher, and there are some adhesive rocks on the fracture surface. The bottom of the fracture surface also appeared bending; The fracture surface of rock sample 6# is even.

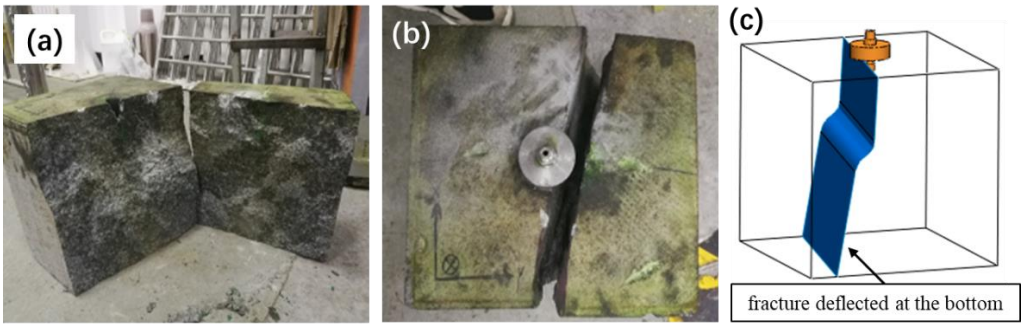

Fig.8 Photo after fracturing and three dimensional diagram after fracturing of rock sample 4#. (a): Photo of the fracture surface after fracturing; (b): Top view of rock sample 3# after fracturing; (c): 3D perspective view of rock sample 3# after fracturing.

The post-fracturing photo of 8# rock sample and the three-dimensional diagram of fracture surface are shown in Fig.9 below. There is a natural fracture and a dike in the rock sample (see Fig.9 (c)), which have a great influence on the propagation of the hydraulic fracture. The results show that the fracture expands in the direction perpendicular to the natural fracture surface and the dike interface under a large stress difference. When the hydraulic fracture tip is close to the dike, the direction will deflect, and then enter the dike, and continue to turn and expand in the dike. When intersecting the natural fracture, the hydraulic fracture is arrested by the natural fracture and spreads along the natural fracture in turn.

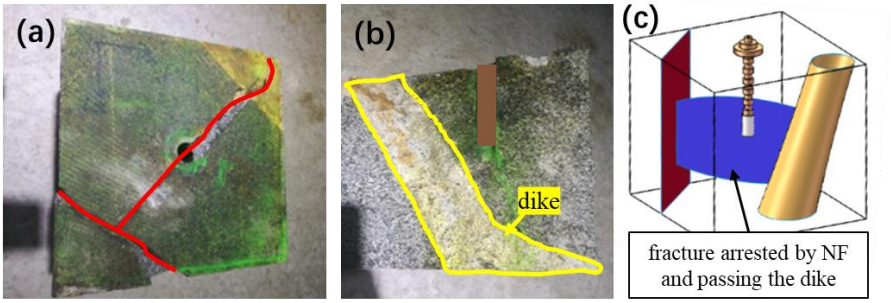

Fig.9 Photo after fracturing and three dimensional diagram after fracturing of rock sample 8#. (a): Photo of the fracture surface after fracturing; (b): Top view of rock sample 3# after fracturing; (c): 3D perspective view of rock sample 3# after fracturing.

The hydraulic pressure curves of the four rock samples during fracturing are shown in Fig.10 below. The results in the figure show that the in-situ stress still has a certain influence on the fracture pressure at high temperature. When the minimum plane stress is unchanged, the larger the difference of plane ground stress is, the smaller the fracture pressure is. By comparing rock samples 4# and 6#, according to the theoretical calculation formula of fracture pressure, the difference of fracture pressure between the two rock samples should be 3MPa, and the experimental result is 3.3MPa, indicating that the influence of temperature on fracture pressure is mainly reflected in the additional thermal stress around the well. When the temperature is the same, this influence will be offset.

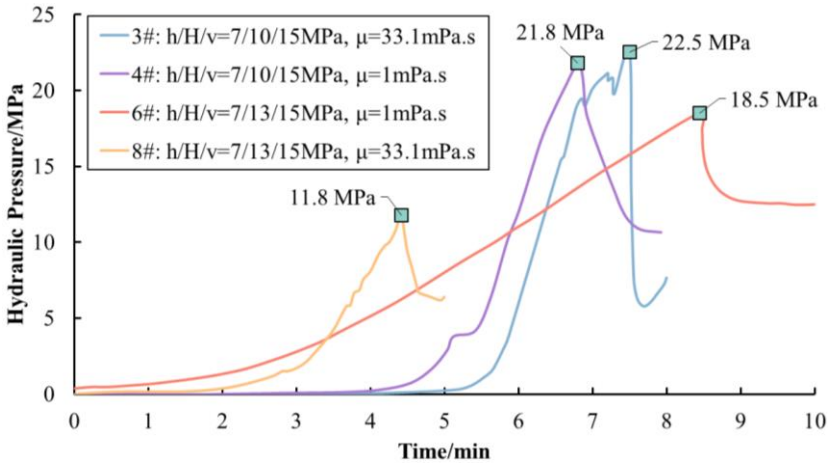

Fig.10 Hydraulic pressure curve of rock samples 3#, 4#, 6# and 8# during fracturing

3.3 Fracturing under different injection rate

Rocks of different lithology and brittleness have different fracture characteristics under different injection velocities. The HDR reservoirs are mostly granite with high brittleness degree, and the response to the change of injection velocity is more obvious. In this section, guar gum was used for fracturing at 200℃ and the same confining pressure, with injection rates of 5 mL/min, 10 mL/min and 30 mL/min, respectively. The parameters used in the simulation are shown in Table 4 below.

Table 4 Experiments parameters used for rock samples 5#、7# and 8#

Index	Temperature (℃)	Confining pressure (h/H/v) (MPa)	Injection rate (mL/min)	Viscosity (mPa·s)
5#	200	7/13/15	5	33.1
7#	200	7/13/15	10	33.1
8#	200	7/13/15	30	33.1

Fig. 11 shows the fracturing results of rock sample 5#. There is no natural fracture in this core, and the fracture propagation trajectory is slightly zigzagging at the injection velocity of 5mL/min, but it mainly expands along the direction of the maximum in-situ stress in the plane, and the fracture surface is rough.

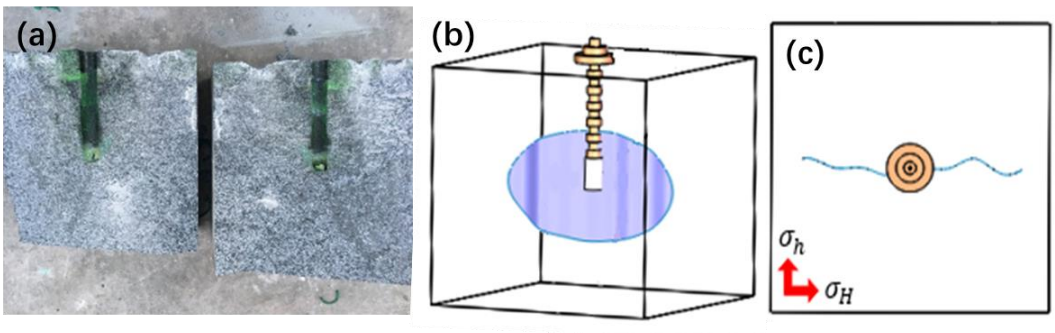

Fig.11 Photo after fracturing and three-dimensional diagram after fracturing of rock sample 5#. (a): Photo of the fracture surface after fracturing; (b): 3D perspective view of rock sample 5# after fracturing; (c): Top view of rock sample 5# after fracturing.

Fig. 12 shows the fracturing results of rock sample 7#. There is a horizontal natural fracture at the bottom of the rock sample. The fracturing results show that this natural fracture seriously affects the expansion of the hydraulic fracture and leads to the diversion of the hydraulic fracture. Compared with the 8# rock sample, which also has natural fractures, the 7# rock sample has a smaller fluid injection rate during fracturing and is more affected by natural fractures.

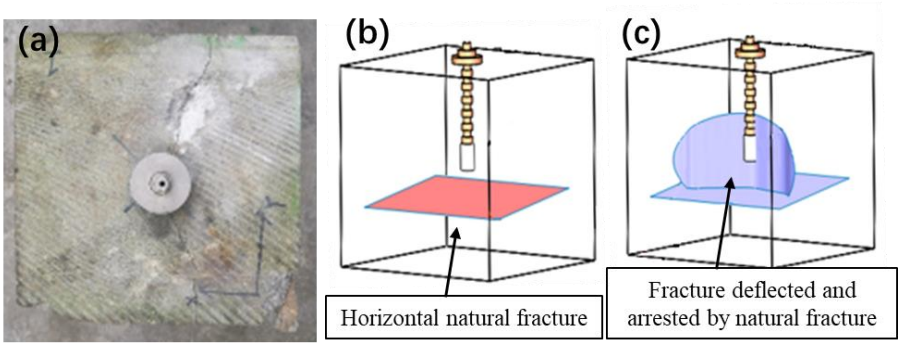

Fig.12 Photo after fracturing and three-dimensional diagram before and after fracturing of rock sample 7#. (a): Photo of the rock sample before fracturing; (b): 3D perspective view of rock sample 7# before fracturing; (c): 3D perspective view of rock sample 7# after fracturing.

4. CONCLUSION

(1). The fracture morphology and the intersection mode of hydraulic fracture and natural fracture in HDR reservoir are influenced by the factors such as temperature, the magnitude and difference of in-situ stress, and fracturing fluids injection rate.

(2). Compared with conventional fracturing, the fracturing of HDR reservoirs is significantly affected by temperature. The higher the temperature, the lower the fracture pressure. And the higher the temperature, the brittleness of rock decreases, and the plasticity increases.

(3). The effects of in-situ stress and fracturing fluids injection rate on HDR reservoir fracturing are similar to those on conventional reservoir fracturing. The experience of conventional formation fracturing can also be used for reference in HDR fracturing operations.

REFERENCES

[1] Cheng Y, Zhang Y, Yu Z, et al. Investigation on Reservoir Stimulation Characteristics in Hot Dry Rock Geothermal Formations of China During Hydraulic Fracturing[J]. ROCK MECHANICS AND ROCK ENGINEERING. 2021, 54(8): 3817-3845.

[2] Zhang W, Wang C, Guo T, et al. Study on the cracking mechanism of hydraulic and supercritical CO2 fracturing in hot dry rock under thermal stress[J]. ENERGY. 2021, 221.

[3] Zhou Z, Jin Y, Zeng Y, et al. Investigation on fracture creation in hot dry rock geothermal formations of China during hydraulic fracturing[J]. RENEWABLE ENERGY. 2020, 153: 301-313.

[4] Yoshida K, Fomin S, Jing Z Z, et al. Dynamics in a complex-fracture-subterranean-system with application to HDR geothermal reservoirs[Z]. 3rd International Symposium on Slow Dynamics in Complex Systems: 2004: 708, 460-461.

[5] Zhang Q. Research and application of artificial fracturing mechanism in enhanced geothermal system[D]. Jilin University, 2014.

[6] Guo L. Experimental and model study on hydraulic fracturing and reservoir damage evolution in enhanced geothermal system[D]. Jilin University, 2016.

[7] Zhou C, Wan Z, Zhang Y, et al. Experimental study on hydraulic fracturing of granite under thermal shock[J]. GEOTHERMICS. 2018, 71: 146-155.

[8] Hou B, Cui Z, Ding J, et al. Perforation optimization of layer-penetration fracturing for commingling gas production in coal measure strata[J]. Petroleum Science. 2022.

[9] Hou B, Chang Z, Wu A, et al. Simulation of competitive propagation of multi-fractures on shale oil reservoir multi-clustered fracturing in Jimsar sag[J]. Acta Petrolei Sinica. 2022, 43(1): 75-90.

[10] Chang Z, Hou B, Ding J. Competitive propagation simulation of multi-clustered fracturing in a cracked shale oil reservoir[J]. Geomechanics and Geophysics for Geo-Energy and Geo-Resources. 2022, 8(3).

[11] Hou B, Dai Y, Zhou C, et al. Mechanism study on steering acid fracture initiation and propagation under different engineering geological conditions[J]. Geomechanics and Geophysics for Geo-Energy and Geo-Resources. 2021, 7(3).

[12] Hou B, Dai Y, Fan M, et al. Numerical simulation of connected hole in acid compression fracture based on phase field method[J]. Acta Petrolei Sinica. 2022, 43(06): 849-859.

[13] Zhang Q, Hou B, Lin B, et al. Integration of discrete fracture reconstruction and dual porosity/dual permeability models for gas production analysis in a deformable fractured shale reservoir[J]. Journal of Natural Gas Science and Engineering. 2021, 93: 104028.

[14] Hou B, Zhang Q, Liu X, et al. Integration analysis of 3D fractures network reconstruction and frac hits response in shale wells[J]. Energy. 2022, 260: 124906.

[15] Gao Y, Chen M, Lin B, et al. Thermal influences on mechanical properties of oil sands[J]. Chinese Journal of Rock Mechanics and Engineering. 2018, 37(11): 2520-2535.

[16] Gao Y, Chen M, Lin B, et al. Modeling of reservoir temperature upon preheating in SAGD wells considering phase change of bitumen[J]. INTERNATIONAL JOURNAL OF HEAT AND MASS TRANSFER. 2019, 144.

[17] Gao Y, Pang H, Jin Y, et al. Evaluation of Shear Dilation Capability/Potential and Permeability Changes in Karamay Oil Sands under Water Injection[J]. GEOFLUIDS. 2019, 2019.

[18] Gao Y, Chen M, Lin B, et al. An analytical model of hydraulic dilation area for Karamay oil sand reservoir under water injection in SAGD wells[J]. JOURNAL OF PETROLEUM SCIENCE AND ENGINEERING. 2019, 179: 1090-1101.

FUNDING:

The authors are grateful for the financial support by the National Key Research and Development Program of China (Grant No.2020YFC1808102) and the Natural Science Foundation of China(No. 51874328 and No. 52074311).

CONFLICTS OF INTEREST:

The authors declare no conflict of interest.